Robotica (2022), **40**, pp. 2527–2546
doi:10.1017/S0263574721001776

CAMBRIDGE
UNIVERSITY PRESS

RESEARCH ARTICLE

Adaptive sliding tracking control for nonlinear uncertain robotic systems with unknown actuator nonlinearities

Shubo Liu*, Guoquan Liu and Shengbiao Wu

Jiangxi Province Engineering Research Center of New Energy Technology and Equipment, East China University of Technology, Nanchang 330013, PR China
*Corresponding author. E-mail: sbliu@ecut.edu.cn

Received: 6 November 2020; **Revised:** 5 October 2021; **Accepted:** 8 November 2021;
First published online: 20 December 2021

Keywords: unknown actuator nonlinearities, nonlinear uncertain robotic systems, adaptive sliding control, robust disturbance observer, robust performance

Abstract

This study is concerned with the tracking control problem for nonlinear uncertain robotic systems in the presence of unknown actuator nonlinearities. A novel adaptive sliding controller is designed based on a robust disturbance observer without any prior knowledge of actuator nonlinearities and system dynamics. The proposed control strategy can guarantee that the tracking error eventually converges to an arbitrarily small neighborhood of zero. Simulation results are included to demonstrate the effectiveness and superiority of the proposed strategy.

1. Introduction

As an essential control unit in the control loop, the actuator is a physical mechanism that converts control strategy to system input. It is noted that the actuator possesses nonlinear characteristics, resulting in serious degradation of the system stability and performance. Recently, the issue of control systems subject to actuator nonlinearities has attracted considerable attention, and corresponding strategies aiming at different actuator nonlinearities have been developed in refs. [1–10]. In refs. [1–3], sliding surface control, robust fuzzy control and fixed-time control are investigated for robotic systems with dead-zone actuator nonlinearity to improve the tracking performances, respectively. In ref. [4], an adaptive controller in the attitude control of flexible spacecraft subject to actuator deadzone is presented under event-triggered mechanism to balance the reduction of communication rate and attitude control performance. Adaptive sliding control approaches for uncertain nonlinear systems preceded by unknown backlash-like hysteresis and Bouc–Wen type of hysteresis nonlinearity are proposed in refs. [5, 6], in which the tracking errors can asymptotically converge to zero. In ref. [7], an adaptive compensation control based on backstepping techniques is proposed for a class of uncertain nonlinear systems preceded by hysteretic actuators with unknown failures. The control problem for the multiple robotic arms with actuator hysteresis and motion constraint is studied in ref. [8], whose motion and internal forces can be guaranteed to converge to the prescribed values by the developed decentralized adaptive fuzzy scheme. In refs. [9, 10], the adaptive tracking control problems are investigated for nonlinear systems with asymmetric actuator backlash and uncertain actuator backlash, respectively. However, they have the main drawback of poor generality since each of them is designed only for a specific type of actuator nonlinearity. As a matter of fact, characteristics of actuator nonlinearity are difficult to obtain accurately, and even completely unknown for designers, which limits their practical applications. Thus, it is of great significance to investigate a unified control approach for unknown actuator nonlinearities. In ref. [11], a robust adaptive control law is designed under the unified framework of hysteresis and dead-zone nonlinearities for stochastic mechanical systems. In refs. [12–14], Nussbaum function-based approach is studied for mechanical systems with

© The Author(s), 2021. Published by Cambridge University Press.

https://doi.org/10.1017/S0263574721001776 Published online by Cambridge University Press

unknown actuator nonlinearities, whereas in refs. [15–17] adaptive control strategies are investigated to deal with the control issue of actuator nonlinearities. To the best of our knowledge, study results on unknown actuator nonlinearities are relatively few, which needs further research in the future.

Since nonlinearity and uncertainty do exist universally in real plants of science and engineering, it is necessary to investigate the control problem for nonlinear uncertain robotic systems (NURSs) suffering from actuator nonlinearities. It is well known that sliding mode control (SMC) has been recognized as one of the effective tools to design robust controllers for nonlinear systems [18]. The most outstanding advantage of SMC is the low sensitivity to system uncertainties and disturbances, which relaxes the necessity of an exact dynamic model. In fact, in SMC design for NURSs subject to unknown actuator nonlinearities, uncertainties as well as disturbances, the following issues need to be noted and tackled. On the one hand, the undesirable chatter problem caused by the discontinuous control signal can deteriorate system performance and also cause wear and tear in mechanical devices, which is expected to be eliminated by control designers in practice. On the other hand, all the issues, such as complex actuator nonlinearities, disturbances and uncertainties, existing in a realistic environment can create considerable difficulty in the control design, especially when all of them are taken into account simultaneously, such that conventional SMC could not meet the complex requirements of NURSs. In summary, it is quite essential to further investigate a novel and practical SMC strategy for NURSs.

In this study, an attempt is thus made to provide an effective robust disturbance observer (RDO)-based adaptive sliding tracking control (ASTC) for NURSs, which gives an attractive proposition and offers the possibility of mitigating the highly undesirable chatter in practical control. Firstly, a composite sliding mode surface designed by combining a linear sliding surface with a differential sliding surface is introduced, and then a chatter-free control input is obtained utilizing the estimate of the lumped uncertainty vector. Secondly, a novel RDO is proposed based on H_∞ and regional pole inequalities, which can be solved by differential evolution (DE)–based linear matrix equalities (LMI) optimization. Finally, a detailed constructive parameter design procedure is introduced to guarantee the tracking performance.

The rest of this study is organized as follows. Section 2 introduces the NURSs to be investigated. In Section 3, ASTC design based on RDO is investigated, and the stable analysis is also presented. In Section 4, control parameters are selected according to the constraint of H_2 performance. Simulation study is conducted in Section 5 to demonstrate the effectiveness and superiority of the proposed strategy. Finally, we conclude our findings in Section 6.

Notation: For a matrix M, M^T denotes its transpose; the notation $M > 0$ (<0) means that M is real symmetric and positive (negative) definite. Also, I is used to denote the identity matrix of appropriate dimensions, and $\mathbf{0}$ is used to denote the zero matrix with appropriate dimensions. In symmetric block matrices, an asterisk * represents a term that is readily inferred by symmetry. The i-th eigenvalue of matrix M is denoted by λ_i. The smallest and largest eigenvalues of matrix M are denoted by $\lambda_{\min}$ and $\lambda_{\max}$, respectively.

Notations used in this paper

$\boldsymbol{d}$	The lumped uncertain vector in robotic system
$\boldsymbol{x_i}$	The state variables of robotic system
$\boldsymbol{x_r}$	**The desired trajectory**
$\boldsymbol{e_i}$	The tracking errors for x_i
$\boldsymbol{s_0}$	A linear sliding surface
$\boldsymbol{s}$	A composite sliding surface
$\boldsymbol{\tau_a}$	The control law to be designed
$\boldsymbol{\varpi}$	The first derivative of τ_a
$\boldsymbol{u}$	The joint torque exerted on the robot
$\boldsymbol{\zeta}$	The unmodelled nonlinear vector
Θ	The positive diagonal matrix
$\boldsymbol{f(x,t)}$, $\boldsymbol{b(x,t)}$, $\boldsymbol{\omega(x,t)}$	The functions in robotic system model
$\overline{\boldsymbol{A}}$, $\overline{\boldsymbol{B}}_1$, $\overline{\boldsymbol{B}}_2$, $\overline{\boldsymbol{C}}_1$	The system matrices in robotic augmented system

https://doi.org/10.1017/S0263574721001776 Published online by Cambridge University Press

2. System model

Consider an n-degree-of-freedom robotic system described in physical coordinates by the following equation:

$$M(r)\ddot{r}(t) + G(r,\dot{r})\dot{r}(t) + H(r) = B(r)u(t) + \Lambda(r,\dot{r},t) \tag{1}$$

where $r, \dot{r} \in R^{n\times 1}$ represent the position and velocity, respectively; $B(r) \in R^{n\times n}$ and $u(t) \in R^{n\times 1}$ denote joint torque exerted on the robot; $\Lambda(r,\dot{r},t) \in R^{n\times 1}$ is the unknown disturbance vector; $M(r) \in R^{n\times n}$ represents the symmetric positive definite inertia matrix; $G(r,\dot{r}) \in R^{n\times n}$ represents the Coriolis and centrifugal matrix; $H(r) \in R^{n\times 1}$ denotes the gravitational force vector.

Let $x_1 = r \in R^{n\times 1}$ and $x_2 = \dot{r} \in R^{n\times 1}$, and then system (1) can be transformed into the following state-space form:

$$\begin{cases} \dot{x}_1 = I_n x_2 \\ \dot{x}_2 = f(x,t) + b(x,t)u(t) + \omega(x,t) \end{cases} \tag{2}$$

where $x = [x_1, x_2]^T \in R^{2n\times 1}$ is the system state vector; $b(x,t) = M^{-1}(x)\cdot B(x) \in R^{n\times n}$; $f(x,t) = -M^{-1}(x)[-G(x,\dot{x})x_2 - H(x)] \in R^{n\times 1}$ and $\omega(x,t) = M^{-1}(x)\cdot\Lambda(x,t) \in R^{n\times 1}$ are unknown nonlinear functions.

It is noted that u is affected by unknown actuator nonlinearities. Therefore, a general actuator model is described mathematically as

$$u = \Theta\tau_a + \zeta \tag{3}$$

where $\tau_a \in R^{n\times 1}$ is the control law to be designed; $\Theta = diag[\chi, \cdots, \chi] \in R^{n\times n}$, and $\chi > 0$ is the user-chosen constant; $\zeta \in R^{n\times 1}$ is the unmodelled nonlinear vector that is assumed to be upper bounded.

By combining the aforementioned actuator nonlinearity in (3), robotic system (1) can then be equivalently converted to the following form:

$$\begin{cases} \dot{x}_1 = I_n x_2 \\ \dot{x}_2 = \Theta\tau_a + d \end{cases} \tag{4}$$

where $d \in R^{n\times 1}$ is the lumped uncertain vector defined as

$$d = (b(x,t) - I_n)\Theta\tau_a + f(x,t) + \omega(x,t) + b(x,t)\zeta \tag{5}$$

Remark 1. It can be noteworthy that the cases of normal operation (as $\zeta = 0$) and actuator nonlinearity (as $\zeta \neq 0$) are covered in the actuator model (3) simultaneously. As $\zeta \neq 0$, Eq. (3) provides a unified mathematical form that is capable of modeling a wide class of actuator nonlinearities. Thus, the actuator model in (3) is more general and of practical significance for control design in this paper.

Remark 2. In fact, actuator nonlinearities can exhibit nonsmooth characteristics, such as hysteresis and deadzone, and other complex smooth characteristics existing in many physical applications. In the subsequent design, complex smooth actuator nonlinearity is considered as the starting point of research, whose result can be applied to the control issue of nonsmooth actuator nonlinearity.

The control objective is to design an effective control input τ_a for system (1) with unknown actuator nonlinearities. After applying the control law, one can obtain that x_1 and x_2 converge to the desired trajectories, respectively. That is $x_1 \to x_r, x_2 \to \dot{x}_r$, where $x_r \in R^{n\times 1}$ means the desired trajectory. Let $e_1 = x_1 - x_r$ and $e_2 = x_2 - \dot{x}_r$ be the tracking errors for x_1 and x_2, respectively. Then according to Eq. (4), the error dynamical system can be described by

$$\begin{cases} \dot{e}_1 = e_2 \\ \dot{e}_2 = \Xi + d \end{cases} \tag{6}$$

where $\Xi = \Theta\tau_a - \ddot{x}_r \in R^{n\times 1}$.

https://doi.org/10.1017/S0263574721001776 Published online by Cambridge University Press

3. Design of RDO

3.1. Proposal of sliding tracking control

First, a linear sliding surface is defined as

$$s_0 = K_1 e_1 + e_2 \in R^{n\times 1} \tag{7}$$

where $K_1 = k_1 I_n \in R^{n\times n}$ with $k_1 > 0$ being the user-chosen constant.

Second, by employing the previously defined linear surface, a composite sliding surface is established as

$$s = \dot{s}_0 + K_2 s_0 \in R^{n\times 1} \tag{8}$$

where $K_2 = k_2 I_n \in R^{n\times n}$, with $k_2 > 0$ being the user-chosen constant. The linear sliding surface s_0 combined with the composite sliding surface s is employed to realize the sliding control. As s reaches zero in finite time, both s_0 and $\dot{s}_0$ are bound to reach zero, and then the tracking errors e_1 and e_2 can asymptotically converge to zero.

Substituting (7) into (8), yields

$$\begin{aligned} s &= K_1\dot{e}_1 + \dot{e}_2 + K_1K_2e_1 + K_2e_2 \\ &= \dot{e}_2 + (K_1 + K_2)e_2 + K_1K_2e_1 \end{aligned} \tag{9}$$

Thus, we can select suitable K_1 and K_2 to realize that the tracking errors have favorable dynamics on the sliding surface.

Substitute (6) into (9), and the ultimate sliding surface can be further described as

$$s = \Theta\tau_a(t) + d + (K_1 + K_2)e_2 + K_1K_2e_1 - \ddot{x}_r \tag{10}$$

In addition, differentiating (10) and using (6), the first time derivative of the sliding surface can be expressed as

$$\begin{aligned} \dot{s} &= \Theta\dot{\tau}_a(t) + \dot{d} + (K_1 + K_2)\Theta\tau_a + (K_1 + K_2)d + K_1K_2e_2 - (K_1 + K_2)\ddot{x}_r - \dddot{x}_r \\ &= \Theta\dot{\tau}_a(t) + \Im v + (K_1 + K_2)\Theta\tau_a + K_1K_2e_2 - (K_1 + K_2)\ddot{x}_r - \dddot{x}_r \end{aligned} \tag{11}$$

where $v = [d^T, \dot{d}^T]^T \in R^{2n\times 1}$ is the vector to be estimated, and $\Im = [K_1 + K_2, I_n] \in R^{n\times 2n}$.

Assumption 1. The desired trajectory x_r and its time derivatives up to the 3rd order are all continuous and bounded.

Following the exponential reaching law approach, [19] the expression related to the control strategy can be formulated as

$$\Theta\dot{\tau}_a + (K_1 + K_2)\Theta\tau_a = -K_1K_2e_2 - \Im\hat{v} + \dddot{x}_r + (K_1 + K_2)\ddot{x}_r - Ks - (\Pi + K)\mathrm{sgn}(s) \tag{12}$$

where $\hat{v} \in R^{2n\times 1}$ is the estimate of v; $K = kI_n \in R^{n\times n}$ and $\Pi = \eta I_n \in R^{n\times n}$ are the user selectable positive definite matrices.

Then, by substituting (12) into (11), one can obtain that

$$\dot{s} = \Im\tilde{v} - Ks - (\Pi + K)\mathrm{sgn}(s) \tag{13}$$

where $\tilde{v} = v - \hat{v}$ is the estimate error vector.

Define the error vector $e = [e_1^T, e_2^T]^T \in R^{2n\times 1}$, and thus an augmented system can be established by taking the control input as an auxiliary state, which is described as

$$\begin{cases} \dot{\bar{e}} = \bar{A}\bar{e} + \bar{B}_1\varpi + \bar{B}_2 d \\ y = \bar{C}_1\bar{e} \end{cases} \tag{14}$$

where $\bar{e} = [e^T, \tau_a^T]^T \in R^{3n\times 1}$, $\varpi = \dot{\tau}_a$, $\bar{A} = \begin{bmatrix} 0 & I_n & 0 \\ 0 & 0 & \Theta \\ 0 & 0 & 0 \end{bmatrix}$, $\bar{B}_1 = \begin{bmatrix} 0 \\ 0 \\ I_n \end{bmatrix}$, $\bar{B}_2 = \begin{bmatrix} 0 \\ I_n \\ 0 \end{bmatrix}$, $\bar{C}_1 = \begin{bmatrix} I_n & 0 & 0 \\ 0 & I_n & 0 \end{bmatrix}$.

https://doi.org/10.1017/S0263574721001776 Published online by Cambridge University Press

Remark 3. In Eq. (12), the discontinuous sign function switch term is diverted into the first derivative of control input, and the actual control input obtained after the integration operation will not consist of any high frequency switching component. Therefore, the actual control input is ultimately smooth and continuous, which is free from chatter phenomenon.

Remark 4. It is obvious that the proposed control law in (12) involves the estimate of the lumped unknown function vector. Hence, it is necessary to establish an effective disturbance observer (DO) to accomplish the control strategy in (12), which will be detailed in Section 3.2.

3.2. Establishment of RDO

The purpose of this section is to design RDO based on H_∞ and pole assignment theories and utilize it to estimate the unknown function vector. Sufficient LMI–based existence conditions will be presented with the following DO:

$$\begin{cases} \hat{v} = p + \aleph e_2 \\ \dot{p} = -\aleph \Xi + Q\hat{v} \end{cases} \tag{15}$$

where $p \in R^{2n\times 1}$, $\aleph \in R^{2n\times n}$ and $Q \in R^{2n\times 2n}$.

Assumption 2. The lumped vector d and its time derivatives up to the second order are continuous and norm bounded, that is,

$$\left\| d^{(j)}(x, t, \tau_a) \right\| \le \mu_j < +\infty, \quad \text{for } j = 0, 1, 2 \tag{16}$$

where μ_j is a positive unknown number.

According to (6) and (15), the derivative of $\hat{v}$ can be expressed as

$$\begin{aligned} \dot{\hat{v}} &= \dot{p} + \aleph \dot{e}_2 \\ &= -\aleph \Xi + Q\hat{v} + \aleph(\Xi + d) \\ &= Q\hat{v} + \aleph d \end{aligned} \tag{17}$$

The estimate error vector $\tilde{v}$ is described as

$$\tilde{v} = v - \hat{v} = \begin{bmatrix} d \\ \dot{d} \end{bmatrix} - \begin{bmatrix} \hat{d} \\ \dot{\hat{d}} \end{bmatrix} = \begin{bmatrix} \tilde{d} \\ \dot{\tilde{d}} \end{bmatrix} \tag{18}$$

Differentiating (18) and using (17), we have

$$\begin{aligned} \dot{\tilde{v}} &= \dot{v} - \dot{\hat{v}} \\ &= Fv + \Psi \ddot{d} - Q\hat{v} + Tv \\ &= Q\tilde{v} + \Psi \ddot{d} \end{aligned} \tag{19}$$

where $F = \begin{bmatrix} 0_{n\times n} & I_{n\times n} \\ 0_{n\times n} & 0_{n\times n} \end{bmatrix}$, $\Psi = \begin{bmatrix} 0_n \\ I_n \end{bmatrix}$, $T = [-\aleph, 0_{2n\times n}]$, $Q = T + F$.

Consequently, by choosing the estimate error as the controlled output, system (19) can be rewritten as

$$\begin{cases} \dot{\tilde{v}} = Q\tilde{v} + \Psi\vartheta \\ z = \tilde{v} \end{cases} \tag{20}$$

where $\vartheta = \ddot{d}$.

The RDO design problem under consideration is to find appropriate matrix Q in (20) such that the error system satisfies the following requirements:

(i) The error system (19) is asymptotically stable, and the H_∞ norm of the closed–loop transfer function from ϑ to z, that is, $||T_{\vartheta z}||_\infty$, should be as small as possible.

https://doi.org/10.1017/S0263574721001776 Published online by Cambridge University Press

(ii) All the system poles in (19) should be located into a specified circular disk $\mathfrak{E}(q_c,r_a)$, which is included in the open left–half complex plane. Here, the circular disk $\mathfrak{E}(q_c,r_a)$ denotes the disk with center at $(-q_c,0)$ and radius r_a, where $q_c > r_a > 0$.

Lemma 1. By virtue of the Bounded Real Lemma [20, 21] for the estimate error system (20), the H_∞ norm of $T_{\vartheta z}$ is less than ρ if and only if there exists a symmetric positive definite $\Sigma_1 \in R^{2n\times 2n}$ with

$$\begin{bmatrix} Q^T\Sigma_1 + \Sigma_1 Q & \Sigma_1\Psi & I \\ * & -\rho I & 0 \\ * & * & -\rho I \end{bmatrix} < 0 \tag{21}$$

Lemma 2. According to literature, [22] all poles of system (20) are located into the specified circular disk $\mathfrak{E}(q_c,r_a)$, if and only if there exists a symmetric positive definite $\Sigma_2 \in R^{2n\times 2n}$ with

$$\begin{bmatrix} -r_a\Sigma_2 & q_c\Sigma_2 + Q\Sigma_2 \\ * & -r_a\Sigma_2 \end{bmatrix} < 0 \tag{22}$$

As a consequence of Lemmas 1 and 2, if matrix inequalities (21) and (22) are satisfied simultaneously, an optimal matrix Q can be obtained via the following minimization problem

$$\begin{aligned} &\min \rho \\ &\text{subject to (21) and (22).} \end{aligned} \tag{23}$$

Hence, the performances (i) and (ii) can be satisfied in system (20) simultaneously.

3.3. Solution for optimization problem of RDO

From the observation of (19), it is easy to find that matrix Q is an additive combination of matrices T and F, leading to certain inconveniences in solving the optimization problem (23) by LMI directly. Furthermore, the assumption of $\Sigma_1 = \Sigma_2$ in (23) can inevitably cause some conservation in traditional LMI method. Thus, it is necessary to introduce a nonconservative algorithm to solve the optimization problem.

DE is a stochastic, population-based algorithm with the advantages of the global solution finding property and powerful search capability, which is firstly proposed by Storn and Price [23, 24]. Hence, a DE-based LMI which combines the effective solution of LMI and the randomized search of DE will be utilized to obtain the optimal matrix Q by solving the optimization problem (23). Since the standard DE can be found in several related refs. [25, 26], the procedures of the proposed optimization algorithm are outlined as follows.

Step 1: Population initialization. An initial population of N_p individuals for $\aleph$ is randomly generated one or more times until every corresponding matrix Q can satisfy the constraint requirement in (23).

Step 2: Objective function evaluation. For any initialized matrix Q, problem (23) turns to LMI which can be efficiently solved by MATLAB LMI Toolbox, and take each ρ as the objective value corresponding to every individual.

Step 3: Evolution process. In this step, three operations of mutation, crossover and selection are implemented in turn to select the optimal individual.

Step 4: If a stopping criterion is satisfied, then output the optimal individual as well as its objective value; otherwise return to Step 2.

Remark 5. In refs. [27, 28], stability analysis is the only concern for DO design. In contrast, techniques of H_∞ disturbance attenuation and pole assignment are integrated into RDO design to improve its performances. Hence, the proposed RDO is more robust for practical implementation.

https://doi.org/10.1017/S0263574721001776 Published online by Cambridge University Press

3.4. Performance analysis for RDO

Since the eigenvalues of Q in system (20) are determined in the left half phase, thus it is always possible to find a positive definite matrix P_ξ such that $Q^T P_\xi + P_\xi Q = -\Phi$ holds for any given positive definite matrix Φ.

Choose the Lyapunov function as $V_1 = \tilde{v}^T P_\xi \tilde{v}$, and then

$$\begin{aligned}\dot{V}_1 =& \dot{\tilde{v}}^T P_\xi \tilde{v} + \tilde{v}^T P_\xi \dot{\tilde{v}} \\ =& \tilde{v}^T (Q^T P_\xi + P_\xi Q)\tilde{v} + 2\tilde{v}^T P_\xi \Psi\vartheta\end{aligned} \tag{24}$$

Noting that

$$2\tilde{v}^T P_\xi \Psi\vartheta \le \frac{1}{\tau}\tilde{v}^T P_\xi P_\xi \tilde{v} + \tau(\Psi\vartheta)^T \Psi\vartheta,$$

where τ is a tunable positive value, the following inequality can be obtained

$$\begin{aligned}\dot{V}_1 &\le -\tilde{v}^T \Phi \tilde{v} + \frac{1}{\tau}\tilde{v}^T P_\xi P_\xi \tilde{v} + \tau(\Psi\vartheta)^T \Psi\vartheta \\ &\le -[\lambda_{\min}(\Phi) - \frac{1}{\tau}\lambda^2_{\max}(P_\xi)]||\tilde{v}||^2 + \tau||\Psi\vartheta||^2\end{aligned} \tag{25}$$

Based on properly chosen Φ, P_ξ and τ, $\lambda_{\min}(\Phi) - \frac{1}{\tau}\lambda^2_{\max}(P_\xi) > 0$ can be guaranteed. It is thus derived that the following inequality

$$\dot{V}_1 \le -\lambda^{-1}_{\max}(P_\xi) \cdot \left[\lambda_{\min}(\Phi) - \frac{1}{\tau}\lambda^2_{\max}(P_\xi)\right] V_1 + \tau||\Psi\vartheta||^2 \le -\gamma_1 V_1 + \gamma_2 \tag{26}$$

where $\gamma_1 = \lambda^{-1}_{\max}(P_\xi) \cdot \left[\lambda_{\min}(\Phi) - \frac{1}{\tau}\lambda^2_{\max}(P_\xi)\right] > 0$ and $\gamma_2 = \tau||\Psi\vartheta||^2 > 0$ hold obviously. Then it can be further obtained that $V_1 \le (V_1(0) - \frac{\gamma_2}{\gamma_1})e^{-\gamma_1 t} + \frac{\gamma_2}{\gamma_1}$, and the norm of the estimation error is upper bounded, that is, $\|\tilde{v}\| \le \bar{L}$.

4. Design of ASTC

4.1. Control law design

In this section, ASTC will be proposed based on RDO designed in Section 3. Substituting (10) into (12) yields

$$\begin{aligned}\Theta\dot{\tau}_a + ((k_1+k_2)+k)\Theta\tau_a =& -KK_1K_2e_1 - (K_1K_2 + KK_1 + KK_2)e_2 - Kd \\ &- \underbrace{(\Im\hat{v} + (\Pi + K)\mathrm{sgn}(s) - \dddot{x}_r - (K_1+K_2+K)\ddot{x}_r)}_{f_s}\end{aligned} \tag{27}$$

where $f_s = (\Im\hat{v} + (\Pi + K)\mathrm{sgn}(s) - \dddot{x}_r - (K_1+K_2+K)\ddot{x}_r)$.

Substituting (27) into (14), one can obtain the following closed–loop augmented system

$$\begin{cases}\dot{\bar{e}} = A_c\bar{e} + B_c\omega_c \\ y = C_c\bar{e}\end{cases} \tag{28}$$

where $A_c = \begin{bmatrix} 0_n & I_n & 0_n \\ 0_n & 0_n & \chi I_n \\ \Upsilon_1 & \Upsilon_2 & \Upsilon_3 \end{bmatrix}$, $B_c = \begin{bmatrix} 0_n & 0_n \\ I_n & 0_n \\ -kI_n/\chi & -I_n/\chi \end{bmatrix}$, $C_c = \begin{bmatrix} I_n & 0_n & 0_n \\ 0_n & I_n & 0_n \end{bmatrix}$, $\omega_c = \begin{bmatrix} d \\ f_s \end{bmatrix}$;
$\Upsilon_1 = -kk_1k_2I_n/\chi$, $\Upsilon_2 = (-k_1k_2 - kk_1 - kk_2)I_n/\chi$, $\Upsilon_3 = (-k - k_1 - k_2)I_n$.

https://doi.org/10.1017/S0263574721001776 Published online by Cambridge University Press

By calculation, one can obtain that $\lambda_{3i-2}(A_c) = -k_1$, $\lambda_{3i-1}(A_c) = -k_2$, $\lambda_{3i}(A_c) = -k$, $i = 1,2,\ldots,n$. Since the eigenvalues are definitely located in the open left–half complex plane, matrix A_c is Hurwitz.

Theorem 1. Considering the nonlinear uncertain system (2), if the system control law is designed as

$$\begin{cases} \tau_a(t) = e^{-(K_1+K_2)t}\tau_a(0) + \int_0^t e^{-(K_1+K_2)(t-\upsilon)}B_\upsilon(t-\upsilon)d\upsilon \\ B_\upsilon = \Theta^{-1}(-K_1K_2e_2 - \Im\hat{v} + \ddot{x}_r + (K_1+K_2)\dot{x}_r - Ks - (\prod + K)\mathrm{sgn}(s)) \end{cases} \tag{29}$$

the controlled system will be globally stable and the tracking errors will converge to zero with the following adaptive laws:

$$\begin{cases} \dot{k} = \alpha||s|| \\ \dot{\eta} = \beta||s|| \end{cases} \tag{30}$$

where α and β are the adaptive rates.

Proof. From (12), it can be obtained that the system control law (29) holds.

Define $\tilde{k}$ and $\tilde{\eta}$ as

$$\tilde{k} = k_0 - k, \quad \tilde{\eta} = \eta_0 - \eta \tag{31}$$

where $k_0 = \eta_0 = ||\Im||\bar{L}/2$.

Choose a Lyapunov function candidate as

$$V = \frac{1}{2}s^Ts + \frac{1}{2\alpha}\tilde{k}^2 + \frac{1}{2\beta}\tilde{\eta}^2$$

It is obvious that V is a positive definite function. Taking the time derivative of the Lyapunov function, candidate V gives

$$\dot{V} = s^T\dot{s} + \frac{1}{\alpha}(k_0 - k)(-\dot{k}) + \frac{1}{\beta}(\eta_0 - \eta)(-\dot{\eta}) \tag{32}$$

In view of Eq. (13), it follows that

$$\begin{aligned} \dot{V} &= s^T\Im\tilde{v} - s^TKs - s^T(\Pi + K)\mathrm{sgn}(s) + \frac{1}{\alpha}(k_0 - k)(-\dot{k}) + \frac{1}{\beta}(\eta_0 - \eta)(-\dot{\eta}) \\ &= s^T\Im\tilde{v} - k||s||^2 - (\eta + k)||s||_1 + \frac{1}{\alpha}(k_0 - k)(-\dot{k}) + \frac{1}{\beta}(\eta_0 - \eta)(-\dot{\eta}) \end{aligned} \tag{33}$$

Taking (30) into (33), one can obtain

$$\begin{aligned} \dot{V} &\le ||s|| \cdot ||\Im|| \cdot ||\tilde{v}|| - k||s||^2 - (\eta + k)||s||_1 - ||s||(k_0 - k) - ||s||(\eta_0 - \eta) \\ &= -k||s||_2^2 - (\eta + k)||s||_1 + (\eta + k)||s|| \\ &\le -k||s||_2^2 \end{aligned} \tag{34}$$

According to Eq. (34), it is clear that $\dot{V} \le 0$ is held. Hence, the proof is completed.

Remark 6. The above analyses are conducted for smooth actuator nonlinearity. As far as nonsmooth actuator nonlinearities with finite nondifferentiable points such as hysteresis, deadzone and backlash are concerned, certain $\hat{\hat{d}}$ in estimate vector $\hat{v}$ on these points is still able to be outputted by the proposed RDO. Independent of actuator nonlinear type, vector $\hat{v}$ obtained by RDO acts as system disturbance in system (28), which needs to be further attenuated to guarantee the good system performance in the following study.

4.2 Control parameter design for H_2 performance

As previously mentioned, ASTC is proposed in Theorem 1, in which an essential step is to choose appropriate control parameters before practical application. In this section, control parameters will be

https://doi.org/10.1017/S0263574721001776 Published online by Cambridge University Press

determined by introducing a constructive design procedure under the prescribed H_2 performance of the closed-loop system to further restrain the adverse effects caused by actuator nonlinearity.

Denote the transfer function from ω_c to y as $T_s = C_c(sI\text{-}A_c)\text{-}[1]\ B_c$. If $\|T_s\|_2$ has an upper bound, then we call that the closed-loop system (28) possesses an H_2 performance. Let $k_1 = k_2 = g > 0$ for the convenience of parameter design, and Υ_1, Υ_2 and Υ_3 in matrix A_c can be reformulated as $\Upsilon_1 = -kg^2 I_n/\chi$, $\Upsilon_2 = (-g^2 - 2gk)I_n/\chi$, $\Upsilon_3 = (-k - 2g)I_n$, respectively.

Remark 7. System (28) is asymptotically stable and has an H_2 performance $\lambda > 0$ if and only if there exists a positive definite symmetric matrix Ω such that

$$\begin{cases} A_c\Omega + \Omega A_c^T + B_c B_c^T < 0 \\ Trace(C_c\Omega C_c^T) < \lambda^2 \end{cases} \tag{35}$$

As is well known, (35) is usually utilized as an effective approach for H_2 performance design [29–31] Unfortunately, A_c, B_c and Ω, existing in an nonlinear form in (35), are all unknown matrices to designers. Therefore, it is difficult to solve (35) directly by using LMI toolbox. To overcome this difficulty, a novel straight-forward approach employing the method of definition is alternatively presented to determine the control parameters under the H_2 performance constraint.

Theorem 2. Define $\alpha = k/g$ as the ratio of k to g. If $k_1 = k_2 = g$ and $\alpha > 1$, it follows that $\sup ||T||_2 = \frac{1}{4g^2}\sqrt{\frac{(7g^4+14g^2+3)n}{g}}$ holds for the closed–loop system (28).

Proof. According to the definition of H_2 norm of a transfer function, [32] $\|T\|_2$ can be easily computed as

$$||T||_2 = \sqrt{\frac{n}{4} \cdot \frac{8g^3 + 6g^2k + 2g + k + 2k^2g^3 + 5kg^4}{kg^3(k^2 + 2kg + g^2)}},\ \ n = 1, 2, 3 \cdots \tag{36}$$

Let $\alpha = k/g$, and (36) can be rewritten as

$$||T||_2 = \sqrt{\frac{n}{4} \cdot \frac{2g^5\alpha^2 + (6g^3 + 5g^5 + g)\alpha + (2g + 8g^3)}{\alpha(\alpha + 1)^2 g^6}} \tag{37}$$

Assume that there exists $\delta > 0$ satisfying $||T||_2^2 \le \delta$, that is,

$$\frac{n}{4} \cdot \frac{2g^5\alpha^2 + (6g^3 + 5g^5 + g)\alpha + (2g + 8g^3)}{\alpha(\alpha + 1)^2 g^6} \le \delta, \forall\alpha > 1 \tag{38}$$

Denote $l(\alpha) = 4\delta g^6\alpha^3 + (8\delta g^6 - 2g^5 n)\alpha^2 + (4\delta g^6 - 6g^3 n - 5g^5 n - gn)\alpha + (-8g^3 n - 2gn)$, and then (38) is equivalent to the following problem

$$l(\alpha) \ge 0, \exists\delta > 0, \forall\alpha > 1 \tag{39}$$

Since $l(0) < 0$ holds obviously, (39) can always hold as long as $l(1) \ge 0$, that is,

$$16\delta g^6 - 7g^5 n - 14g^3 n - 3gn \ge 0 \tag{40}$$

By solving inequality (40), δ is obtained as

$$\delta \ge \frac{(7g^4 + 14g^2 + 3)n}{16g^5} \tag{41}$$

Hence, the proof is completed.

Remark 8. Based on the aforementioned analysis, an approach for choosing appropriate control parameters is presented in Theorem 2. It is obvious that $\sup\|T\|_2$ is merely dependent on the user-chosen parameter g, which can be easily determined by solving the inequality $\sup ||T||_2 < \lambda$ for any given $\lambda > 0$. Subsequently, parameter k can then be independently selected to satisfy the constraint of $\alpha > 1$. Thus, the asymptotic stability and the prescribed H_2 performance can be guaranteed simultaneously.

https://doi.org/10.1017/S0263574721001776 Published online by Cambridge University Press

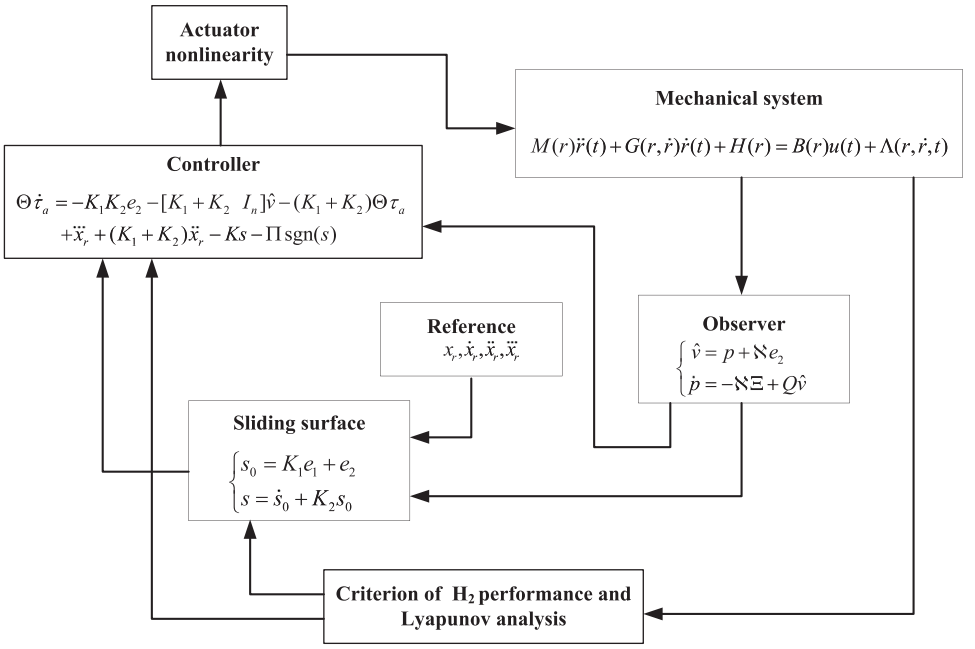


Figure 1. *Block diagram of the proposed control strategy.*

Based on the design process explained in Sections 3 and 4, the block diagram of ASTC is presented in Fig. 1 and the whole flow chart of the algorithm is shown in Fig. 2.

5. Simulation study

In this section, three examples are presented to validate the effectiveness of the proposed control strategy.

5.1. Design procedure

To summarize the analyses in Sections 3 and 4, the procedures of ASTC are outlined as follows:

Step 1. Selection of observer parameters. Setting $q_c = 200$ and $r_a = 100$, and using LMI toolbox of MATLAB to solve minimization problem (23), one can obtain the following optimal DO matrix

$$Q=\begin{bmatrix}-250.87 & 1\\ -19951 & 0\end{bmatrix}. \tag{42}$$

Step 2. Selection of control parameters. Assume that the prescribed H_2 performance is 0.5, and control parameters $k_1$and k_2 are selected as $k_1 = k_2 = 3$. The initial values of k and η are set as $k(0) = 4$ and $\eta(0) = 0$. In addition, adaptive rates $\alpha = 0.03$ and $\beta = 0.01$ are chosen.

5.2. Example 1: System without actuator nonlinearity.

In this section, one-link robotic manipulator system without actuator nonlinearity is considered for tracking its equilibrium point $x_e = [0, 0]^T$ in two cases. Thus, in model (3), $\Theta = 1$ and $\zeta = 0$ are selected for simulation. The system initial state is selected as $x(0) = [0, 1]^T$.

https://doi.org/10.1017/S0263574721001776 Published online by Cambridge University Press

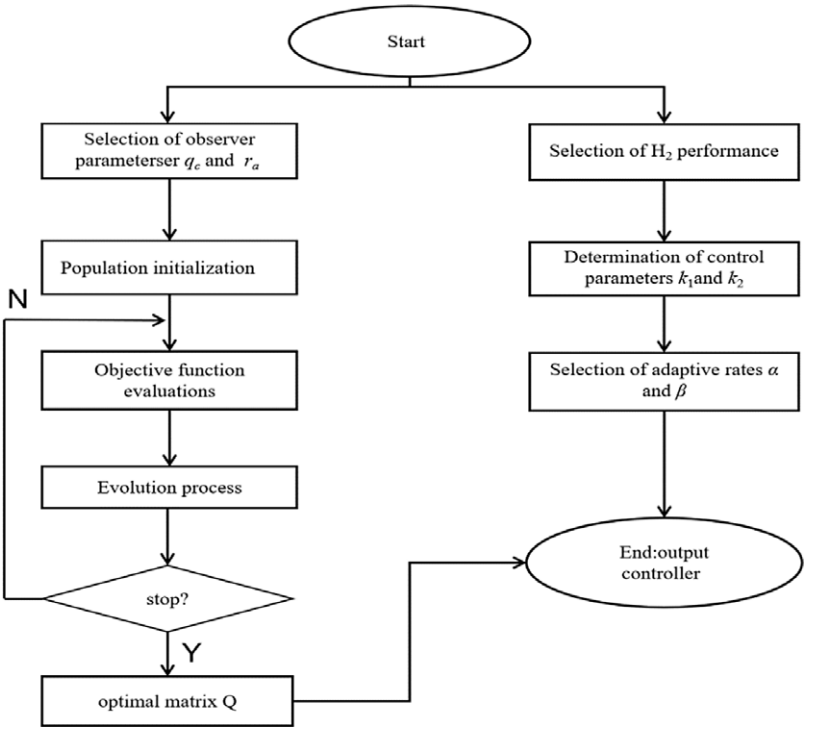


Figure 2. *Flow chart of the proposed adaptive sliding tracking control.*

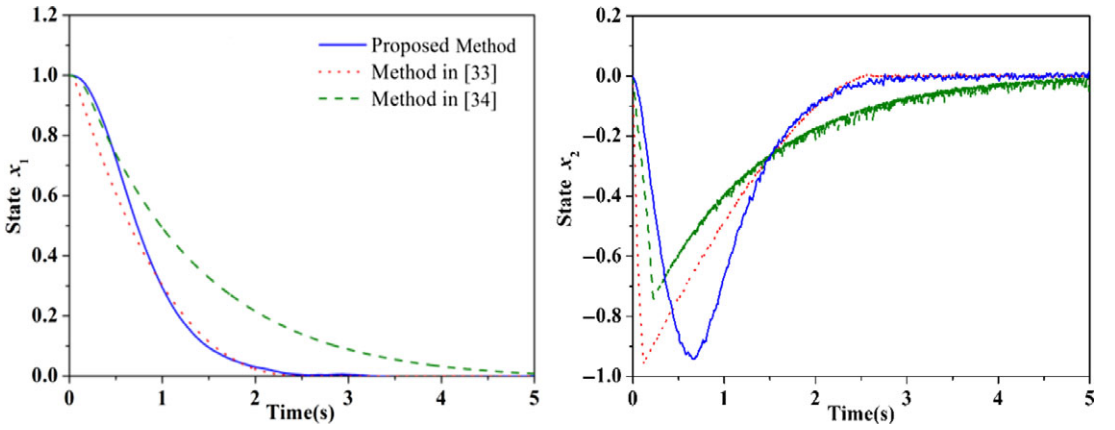


Figure 3. *States x_1 and x_2 for Case 1 in Example 1.*

• Case 1: Nominal system.

System (2) is employed for simulation with $f(x,t) = -x_1^2 - 5x_2$, $b(x,t) = x_1x_2 + 1$ and $\omega(x,t) = (x_1x_2 + 1)(0.2(t-3) + 0.8\sin(3t-3) + 0.5e^{-t}) + \Gamma(t)$, where $\Gamma(t)$ is a random noise of 0 mean and 0.5 variance.

It is observed from Figs. 3 and 4 that the proposed controller can stabilize the considered system quickly. Moreover, no chatter phenomenon can be observed in the control input in Fig. 4. In order to further validate the superiority and effectiveness of the proposed ASTC, the existing results in literature [33, 34] are presented for the objective of comparison.

https://doi.org/10.1017/S0263574721001776 Published online by Cambridge University Press

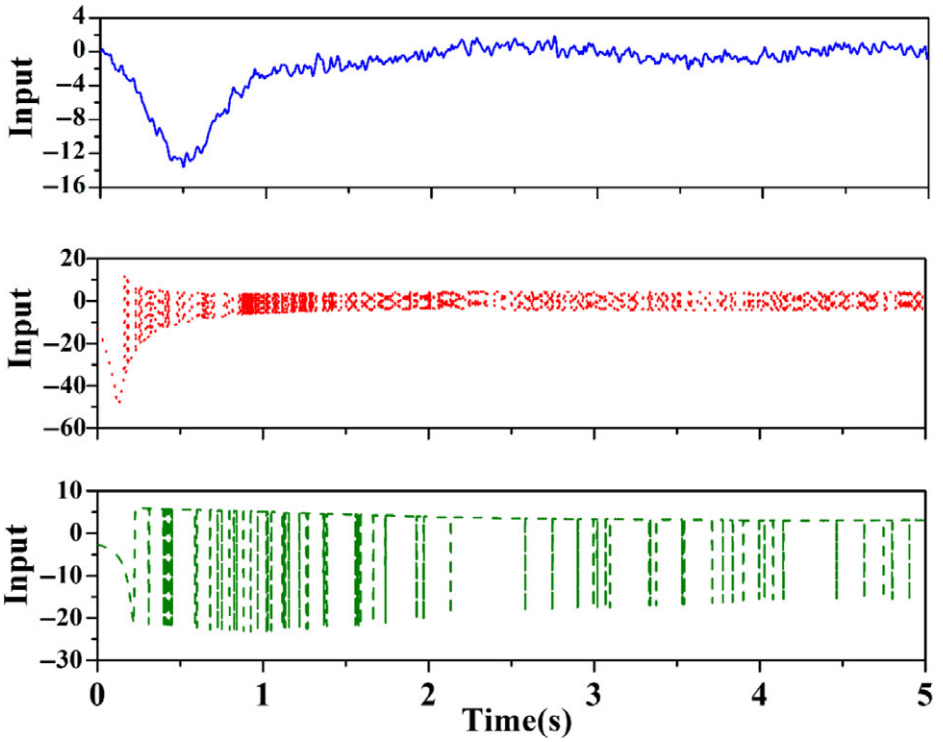


Figure 4. *Control inputs for Case 1 in Example 1.*

The proposed controller is firstly compared with nonsingular terminal sliding mode (NTSM) controller designed in ref. [33] where $b(x,t)$ and $f(x,t)$ are assumed to be precisely obtained. From Fig. 3, we can see that both of the controllers can stabilize the system to the equilibrium state at the same rate, although NTSM control has the outstanding advantage of fast convergence rate by using an enhanced nonlinear sliding surface. However, NTSM controller exhibits serious chatter phenomenon in the control input and substantial increase in the control effort than that in the proposed ASTC in Fig. 4.

For comparison purpose, another class of sliding mode controller in ref. [34] is also considered in the simulation study, in which a robust adaptive sliding (RAS) control based on radial basis function neural networks (RBFNN) is put forward. Different from NTSM controller in ref. [34], the estimates of $b(x,t)$ and $f(x,t)$ by RBFNN are employed in ref. [34], whereas the upper bound of $\xi(x,t)$ is still a necessary requirement. Hence, RAS controller cannot avoid the dependence on prior information on system dynamics. As can be seen in Fig. 3, the system states under controller [34] converge to zero with the slowest rate. In addition, the controller proposed in ref. [34] is also seriously affected by the undesirable chatter phenomenon.

In conclusion, by comparison with the other two SMC-based strategies, similar or better output performances can be achieved although no prior knowledge about the robotic manipulator can be employed in ASTC. Additionally, the proposed controller produces smooth control input with small control efforts, which is free from undesirable chatter phenomenon. Thus, ASTC is appropriate for real applications to NURSs from a practical point of view.

• Case 2: Perturbed system.

In this section, complex changes in $f(x,t)$ and $b(x,t)$ are taken into account to further demonstrate the effectiveness and practicability of ASTC. To this end, a piece-wise nonlinear function of time $\hbar(t)$ is

https://doi.org/10.1017/S0263574721001776 Published online by Cambridge University Press

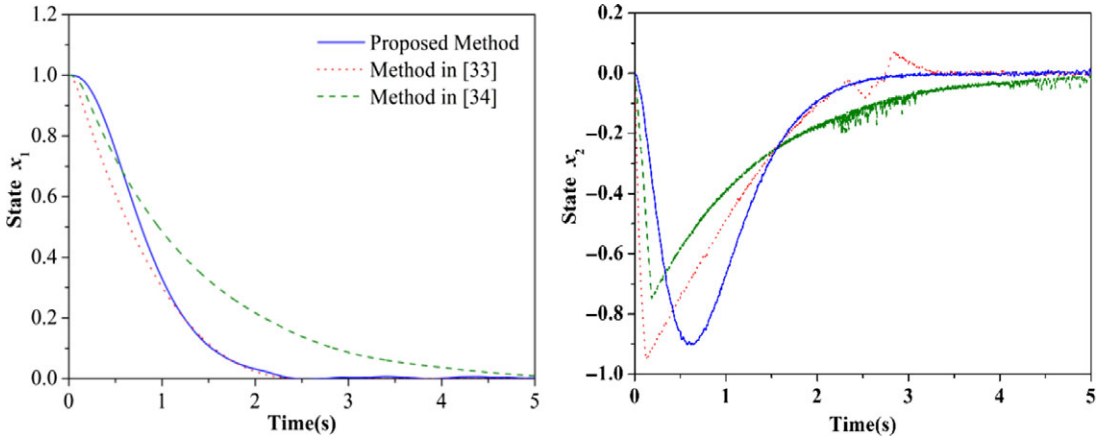


Figure 5. *States x_1 and x_2 for Case 2 in Example 1.*

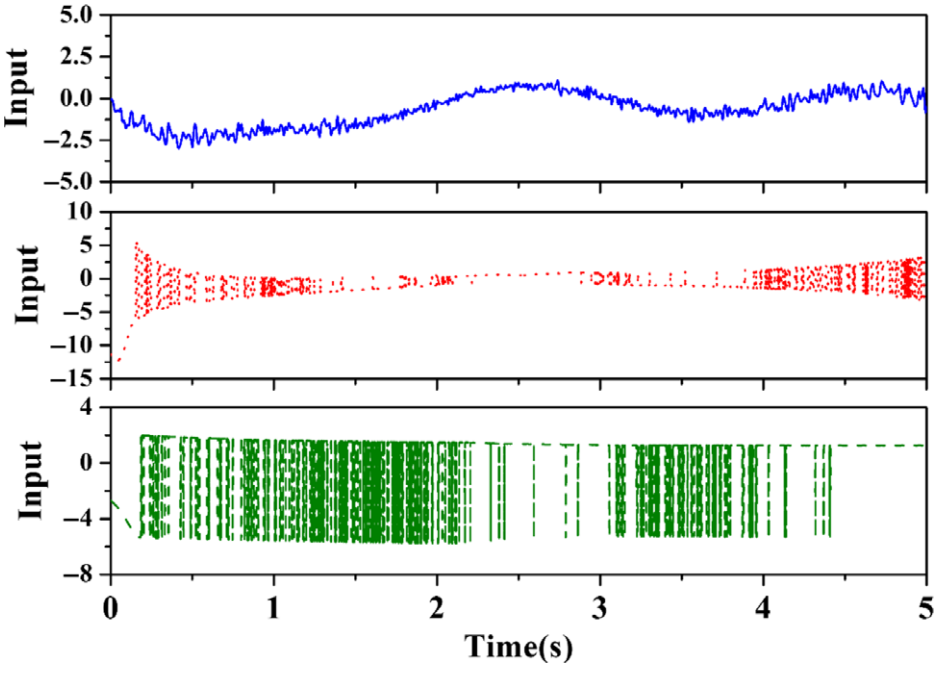


Figure 6. *Control inputs for Case 2 in Example 1.*

introduced as follows:

$$\hbar(t) = \begin{cases} 0.2 + 2t, & 0 \le t \le 2 \\ 5e^{2-t} + 2\sin(0.2\pi t), & 2 \le t \le 4 \\ 3\cos(0.2\pi(t-6)) \cdot \sin(0.3\pi t), & t > 4 \end{cases} \tag{43}$$

According to (43), $f(x, t)$ and $b(x, t)$ are transformed as $f(x, t) = \hbar(t) \cdot (-x_1^2 - 5x_2)$ and $b(x, t) = (x_1 x_2 + 1) + \hbar(t)$, and the output responses are presented in Figs. 5 and 6. It is noteworthy that ASTC can still offer satisfying output performances by applying a smooth control input as compared to the controllers in refs. [33, 34].

https://doi.org/10.1017/S0263574721001776 Published online by Cambridge University Press

Table I. *Performance comparison of control inputs in Example 1.*

	Case 1		Case 2	
Controller	**Control energy**	**TV**	**Control energy**	**TV**
Proposed Adaptive sliding tracking control	80.92	177.97	26.92	135.32
Method in ref. [33]	196.76	1868.30	56.74	448.09
Method in ref. [34]	124.14	793.14	47.35	445.32

To evaluate the smoothness of the control input, the total variance (TV) [35] of the control input is utilized, which is calculated as follows:

$$TV = \sum_{i=1}^{n^{\dagger}-1} |u_{i+1} - u_i| \tag{44}$$

where $n^{\dagger}$ is the number of samples. In addition, energy of the control input is calculated by the 2–norm method. It is obvious that both TV and control input energy are desired to be as small as possible.

Table I shows TV and energy of the system inputs obtained by different control strategies in Cases 1 and 2, which are calculated for the period from 0 to 5 s with a sampling time of 0.01 s. It is clear that the proposed ASTC is able to produce a smoother control input with minimal control energy in both cases.

5.3. Example 2: System with typical actuator nonlinearities.

In this section, another one-link robotic manipulator of system (2) subject to typical actuator nonlinearities is employed, in which

$$\begin{cases} f(x,t) = -x_2 + 3.5x_2^2 \cos x_1 - 35 \sin x_1 \\ b(x,t) = 1 \\ w(x,t) = 0.8e^{-0.2t} \sin t \end{cases} \tag{45}$$

The desired trajectories are described as $x_r = 0.5(\sin t + \sin(0.5t))$ rad and $\dot{x}_r = 0.5(\cos t + 0.5\cos(0.5t))$ rad/s, respectively. The system initial state is selected as $x(0) = [0, 0]^T$. The ASTC parameters carried out in this example are same as those in Example 1, and three different types of actuator nonlinearities are considered. For the objective of comparison, the existing results in ref. [12] are also presented, in which a Nussbaum gain-based adaptive neural network control is fit to the cases that were applied on it.

- Case 1: Actuator with dead-zone nonlinearity described as

$$u = \begin{cases} (1 + 0.3\sin\tau_a)(\tau_a - 0.5), \tau_a \geq 0.5 \\ 0, -0.3 \leq \tau_a \leq 0.5 \\ (0.8 + 0.2\cos\tau_a)(\tau_a + 0.3), \tau_a \leq -0.3 \end{cases} \tag{46}$$

- Case 2: Actuator with hysteresis nonlinearity described as

$$\frac{du}{dt} = \left|\frac{d\tau_a}{dt}\right| (3.2\tau_a - u) + 0.4\frac{d\tau_a}{dt} \tag{47}$$

- Case 3: Actuator with backlash nonlinearity described as

$$u = \begin{cases} 1.2(\tau_a - 0.5), \ \dot{u} > 0 \\ 1.2(\tau_a + 0.6), \ \dot{u} < 0 \\ u(t_-), \ otherwise \end{cases} \tag{48}$$

https://doi.org/10.1017/S0263574721001776 Published online by Cambridge University Press

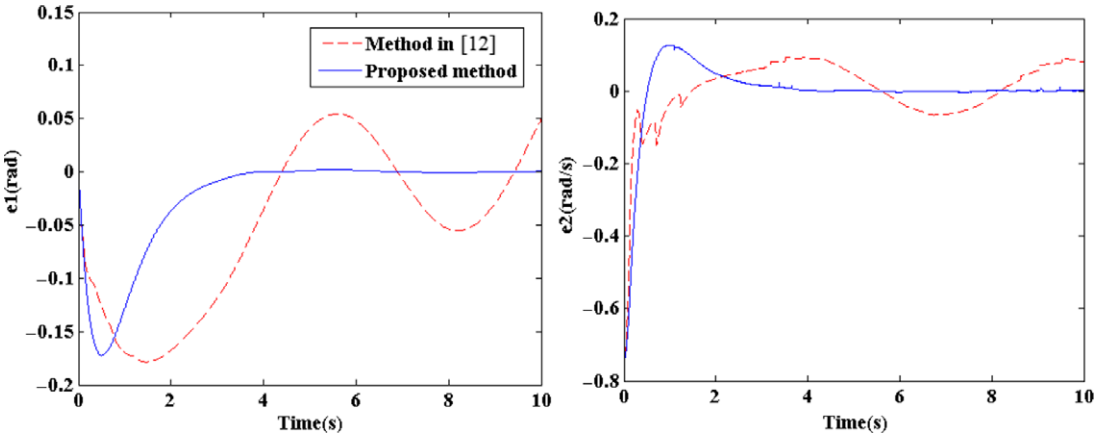


Figure 7. *Tracking errors with dead-zone actuators.*

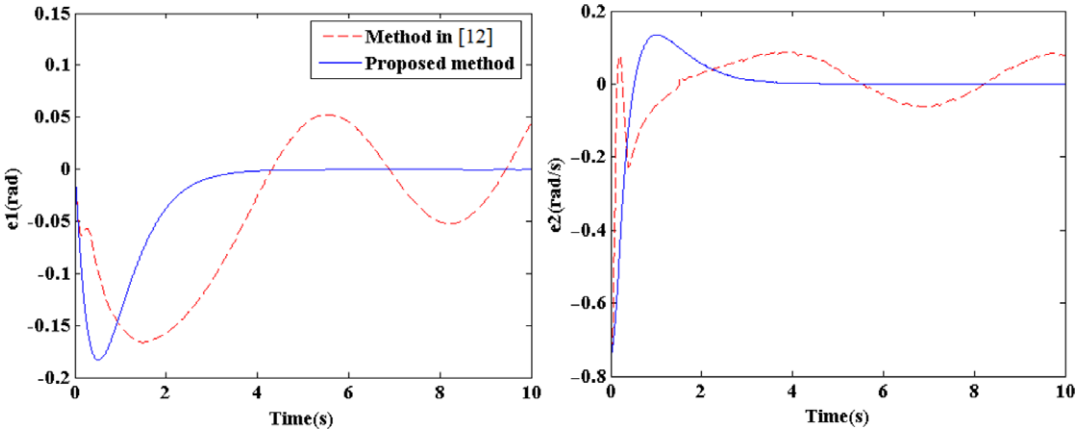


Figure 8. *Tracking errors with hysteresis actuators.*

Simulation results in Figs. 7–9 indicate that the proposed ASTC shows a faster convergence speed and smaller steady-state error when compared with the method in ref. [12]. Thus, ASTC can achieve better tracking performance no matter what the actuator nonlinearities are.

5.4. Example 3: System with complex nonlinearity.

• Case 1: Two-link robot system

In this case, a two-link robotic arm in ref. [13] is employed to confirm the effectiveness of the proposed scheme in this study. The dynamics is described as

$$\begin{bmatrix} M_{11} & M_{12} \\ M_{21} & M_{22} \end{bmatrix} \begin{bmatrix} \ddot{r}_1 \\ \ddot{r}_2 \end{bmatrix} + \begin{bmatrix} G_{11} & G_{12} \\ G_{21} & G_{22} \end{bmatrix} \begin{bmatrix} \dot{r}_1 \\ \dot{r}_2 \end{bmatrix} = \begin{bmatrix} u_1 \\ u_2 \end{bmatrix},$$

where $M_{11} = \xi_1 + 2\xi_3 \cos(r_2)$, $M_{12} = M_{21} = \xi_2 + \xi_3 \cos(r_2) + \xi_4 \sin(r_2)$, $M_{22} = \xi_2 G_{11} = (-\xi_3 \sin(r_2) + \xi_4 \cos(r_2))\dot{r}_2$, $G_{12} = (-\xi_3 \sin(r_2) + \xi_4 \cos(r_2))(\dot{r}_1 + \dot{r}_2)$, $G_{21} = (\xi_3 \sin(r_2) - \xi_4 \cos(r_2))\dot{r}_1$ and $G_{22} = 0$ with actual physical parameters defined as $\xi = [\xi_1, \xi_2, \xi_3, \xi_4]^T = [3.3, 0.97, 1.04, 0.6]^T$. The desired joint and velocity trajectories are chosen as $x_r = \begin{bmatrix} 0.2\sin(t) + 0.1\cos(2t) \\ -0.3\sin(t) - 0.1\cos(2t) \end{bmatrix}$ rad and

https://doi.org/10.1017/S0263574721001776 Published online by Cambridge University Press

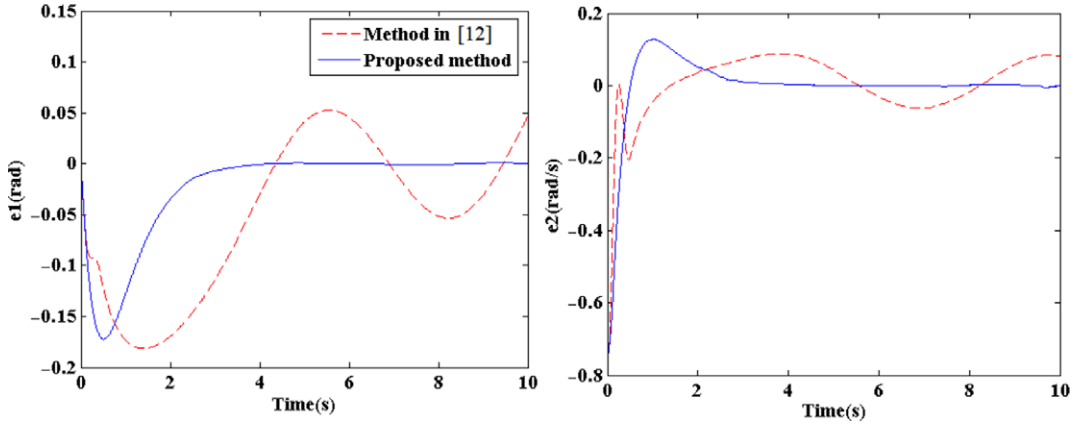


Figure 9. *Tracking errors with backlash nonlinearity actuators.*

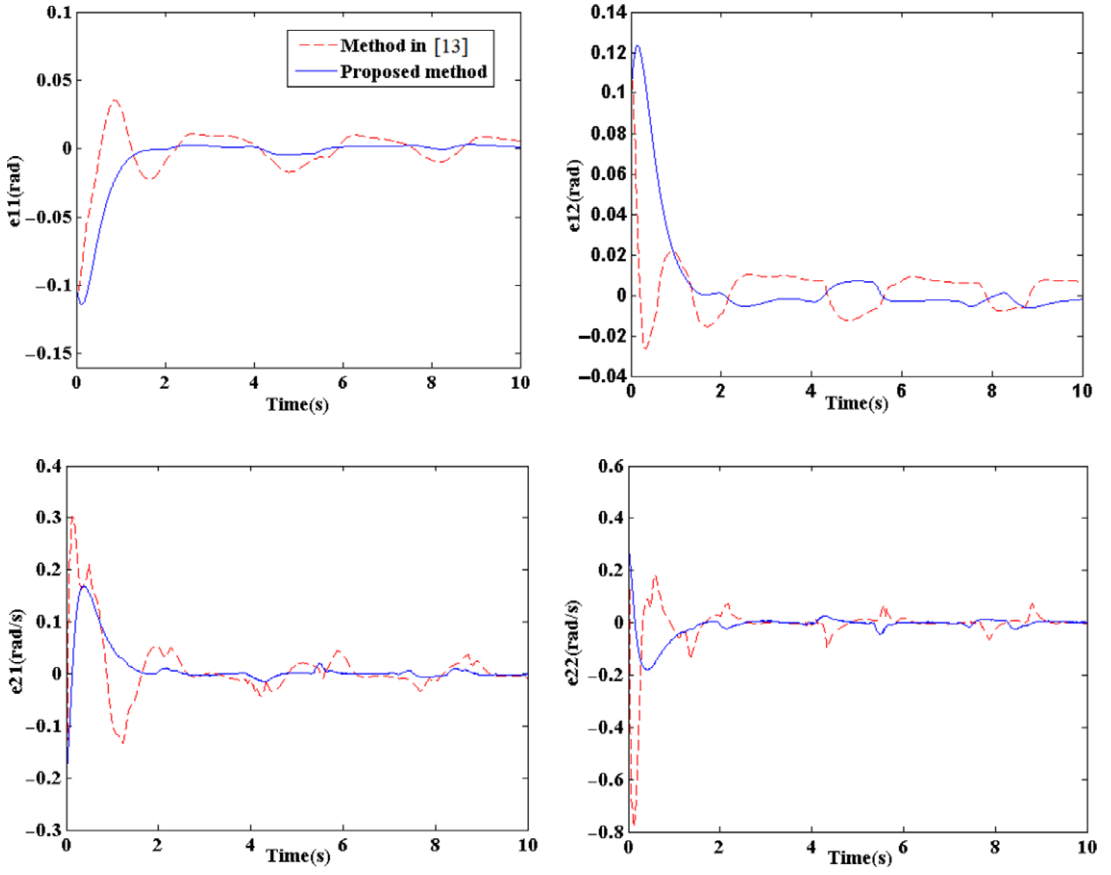


Figure 10. *Tracking errors with complex nonlinearity actuators.*

$\dot{x}_r = \begin{bmatrix} 0.2\cos(t) - 0.2\sin(2t) \\ -0.3\cos(t) + 0.2\sin(2t) \end{bmatrix}$ rad/s, respectively. The initial joint and velocity of the robotic arm are set as $r(0) = [0, 0]^T$ rad and $\dot{r}(0) = [0, 0]^T$ rad/s. Gains in sliding surface are designed as $K_1 = K_2 = 4I_2$, $\Theta = 0.1\, I_2$ and $Q = \begin{bmatrix} -250.87I_2 & I_2 \\ -19951I_2 & 0_2 \end{bmatrix}$. The initial values of k and η are set as $k(0) = 10$

https://doi.org/10.1017/S0263574721001776 Published online by Cambridge University Press

Table II. *Integral of absolute error (IAE) comparison of typical actuator nonlinearities in Example 2.*

	Dead-zone IAE		**Hysteresis IAE**		**Backlash IAE**	
	e_1	e_2	e_1	e_2	e_1	e_2
Adaptive sliding tracking control	0.24	0.35	0.25	0.37	0.24	0.35
Method in ref. [12]	0.72	0.62	0.65	0.60	0.71	0.61

Table III. *Integral of absolute error (IAE) comparison of complex actuator nonlinearity in Case 1 in Example 3.*

	IAE			
	e_{11}	e_{12}	e_{21}	e_{22}
Adaptive sliding tracking control	0.09	0.10	0.16	0.20
Method in ref. [13]	0.11	0.10	0.30	0.32

and $\eta(0) = 0$, respectively. Moreover, adaptive rates $\alpha = 0.03$ and $\beta = 0.01$ are chosen. The complex unknown actuator nonlinearity is simulated as

$$u = \begin{cases} (2 + 0.1\cos(\tau_a))(\tau_a - 0.35), \tau_a \geq 0.35 \\ e^{-2t} + 0.2, \ -0.45 < \tau_a < 0.35 \\ (2 - 0.8\sin(\tau_a))(\tau_a + 0.45), \tau_a \leq -0.45 \end{cases} \tag{49}$$

Joint and velocity tracking errors of the robotic arm are presented in Fig. 10. Moreover, the results of an adaptive method based on new Nussbaum analysis for Multi-Input Multi-Output (MIMO) mechanical systems with unknown actuator nonlinearities in ref. [13] are also given for the sake of comparison. It can be obviously observed that smaller steady-state errors are obtained from Fig. 10, illustrating the effectiveness and superiority of the proposed control approach in dealing with complex actuator nonlinearity.

Integral of absolute error (IAE) values of the tracking errors in Examples 2 and 3 are concluded in Tables II and III, respectively. It is evident that IAE values of ASTC are less than those of the methods provided in refs. [12, 13] correspondingly, showing smaller steady-state errors and better tracking performances.

• Case 2: Single-link robot system

In this case, a single-link robotic arm in ref. [36] is utilized to verify the effectiveness and validity of ASTC. For ease of comparison studies, both the desired joint trajectory and the complex actuator nonlinearity existing in the robot in ref. [36] are utilized for simulation, which are described as

$$x_r = \begin{cases} 0.5\sin\left(\frac{2}{5}\pi t\right), t \leq 15, \\ 0, t > 15. \end{cases} \tag{50}$$

and $u = (1 + 0.3\sin(\tau_a)) \cdot \tau_a$ rad, respectively. Gains in sliding surface are designed as $K_1 = K_2 = 6I_2$, $\Theta = 0.1I_2$ and $Q = \begin{bmatrix} -250.87I_2 & I_2 \\ -19951I_2 & 0_2 \end{bmatrix}$, and the simulation results are presented in Figs. 11 and12. From Fig. 11, it can be observed that ASTC has better tracking effect when compared with the proposed tracking controller in ref. [36]. Furthermore, ASTC is able to eliminate the undesired chattering effectively with less control inputs in Fig. 12, demonstrating great advantages in coping with NURSs with unknown actuator nonlinearities.

https://doi.org/10.1017/S0263574721001776 Published online by Cambridge University Press

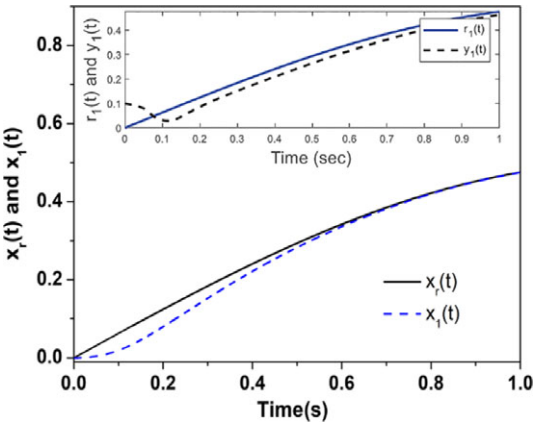


Figure 11. *The trajectories of $x_r(t)$ and $x_1(t)$. Inset: The trajectories of the pre-specified reference $r_1(t)$ and displacement $y_1(t)$ by using the proposed tracking controller [36].*

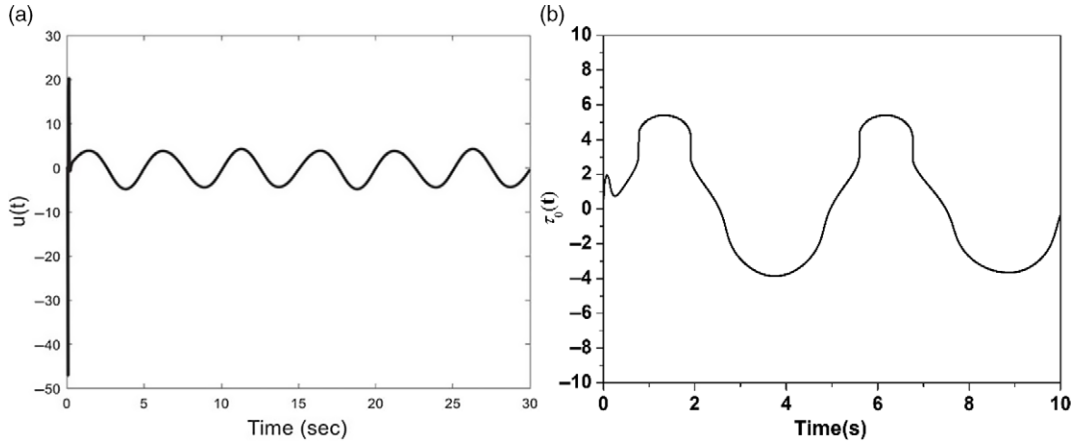


Figure 12. *(a) The control input responses of the proposed continuous tracking controller [36]. (b) The control input responses of adaptive sliding tracking control.*

6. Conclusion

In this study, a RDO-based chatter–free adaptive sliding control is proposed for NURSs with unknown actuator nonlinearities. An additional control parameter scheme is developed to meet the requirement of H_2 performance. The design and implementation of the adaptive control law are conducted without any prior knowledge on actuator nonlinearities and system dynamics. Simulation results can convincingly demonstrate that ASTC can successfully guarantee the tracking error in an arbitrarily small neighborhood of zero, which affirms the effectiveness and superiority of the proposed strategy. From the analyses in Section 4, ASTC with inappropriate parameters can result in degradation of the tracking performances, and thus the control parameter design can play an important role in improving system performance. In future work, a novel design procedure for control parameters will be investigated under the system constraints of H_2, generalized H_2 and H_∞ norms to further improve the system robustness and dynamic performance.

Acknowledgments. The work is financially supported by Jiangxi Provincial Natural Science Foundation (20202BAB202008) and Foundation of Education Department of Jiangxi Province (GJJ170484) and the East China University of Technology Research

https://doi.org/10.1017/S0263574721001776 Published online by Cambridge University Press

Foundation for Advanced Talents (DHBK2019178). The author would like to thank the editor and anonymous reviewers for their helpful comments and suggestions to improve the quality of this study.

Conflicts of Interest. The authors declare that there is no conflict of interest.

References

[1] S. I. Han and J. Lee, "Finite-time sliding surface constrained control for a robot manipulator with an unknown deadzone and disturbance," *ISA Trans*. **65**, 307–318 (2016).
[2] Y. Jiang, Z. Liu, C. Chen and Y. Zhang, "Adaptive robust fuzzy control for dual arm robot with unknown input deadzone nonlinearity," *Nonlinear Dyn.* **81**(3), 1301–1314 (2015).
[3] D. Zhang, L. Kong, S. Zhang, Q. Li and Q. Fu, "Neural networks-based fixed-time control for a robot with uncertainties and input deadzone," *Neurocomputing* **390**, 139–147 (2020).
[4] Q. Liu, M. Liu, Y. Shi and J. Yu, "Event-triggered adaptive attitude control for flexible spacecraft with actuator nonlinearity," *Aerosp. Sci. Technol*. **106,** 106111 (2020).
[5] X. Y. Zhang and Y. Lin, "A robust adaptive dynamic surface control for nonlinear systems with hysteresis input," *Acta Autom. Sin.* **36**(9), 1264–1271 (2010).
[6] J. Zhou, C. Wen and T. Li, "Adaptive output feedback control of uncertain nonlinear systems with hysteresis nonlinearity," *IEEE Trans. Autom. Control* **57**(10), 2627–2633 (2012).
[7] J. Cai, C. Wen and H. Su, "Adaptive inverse control for parametric strict feedback systems with unknown failures of hysteretic actuators," *Int. J. Robust Nonlinear Control* **25**(6), 824–841 (2015).
[8] Z. Liu, C. Chen, Y. Zhang and C. L. P. Chen, "Coordinated fuzzy control of robotic arms with actuator nonlinearities and motion constraints," *Inf. Sci.* **296**, 1–13 (2015).
[9] Y. Zheng and G. Zhang, "Quantized adaptive tracking control for nonlinear systems with actuator backlash compensation," *J. Franklin Inst.* **365**(15), 8484–8506 (2019).
[10] Z. Lyu, Z. Liu, K. Xie, C. L. P. Chen and Y. Zhang, "Adaptive tracking control for switched nonlinear systems with fuzzy actuator backlash," *Fuzzy Sets Syst.* **385**, 60–80 (2020).
[11] H. Pan, W. Sun and X. Jing, "Adaptive tracking control for stochastic mechanical systems with actuator nonlinearities," *J. Franklin Inst.* **354**(7), 2725–2741 (2017).
[12] Z. C. Liu, X. M. Dong, J. P. Xue and L. P. Zhang, "Adaptive control for a class of nonlinear systems with uncertain actuator nonlinearity," *J. Syst. Eng. Electron.* **37**(1), 163–168 (2015).
[13] C. Chen, Z. Liu, Y. Zhang, C. L. P. Chen and S. Xie, "Adaptive control of MIMO mechanical systems with unknown actuator nonlinearities based on the Nussbaum Gain Approach," *IEEE/CAA J. Autom. Sinica* **3**(1), 26–34 (2016).
[14] C. Chen, Z. Liu, Y. Zhang, C. L. P. Chen and S. Xie, "Saturated Nussbaum function based approach for robotic systems with unknown actuator dynamics," *IEEE Trans. Cybern.* **46**(10), 2311–2322 (2016).
[15] C. Chen, Z. Liu, Y. Zhang and C. L. P. Chen, "Adaptive control of robotic systems with unknown actuator nonlinearities and control directions," *Nonlinear Dyn.* **81**(3), 1289–1300 (2015).
[16] Z. Liu, C. Chen, Y. Zhang and C. L. P. Chen, "Adaptive neural control for dual-arm coordination of humanoid robot with unknown nonlinearities in output mechanism," *IEEE Trans. Cybern.* **45**(3), 507–518 (2015).
[17] X. Hu, L. Wu, X. Si and C. Hu, "Adaptive tracking control of MIMO nonlinear nonminimum phase system with unknown input nonlinearity," *Int. J. Robust Nonlinear Control* **28**(2), 596–610 (2018).
[18] J. Y. Hung, W. Gao and J. C. Hung, "Variable structure control: A survey," *IEEE Trans. Ind. Electron*. **40**(1), 2–22 (1993).
[19] K. B. Devika and S. Thomas, "Sliding mode controller design for MIMO nonlinear systems: a novel power rate reaching law approach for improved performance," *J. Franklin Inst.* **355**(12), 5082–5098 (2018).
[20] H. Chen and K. H. Guo, "Constrained H_∞ control of active suspensions: An LMI approach," *IEEE Trans.* Control Syst. *Technol.* **13**(3), 412–421 (2005).
[21] E. Prempain and I. Postlethwaite, "Static output feedback stabilization with H_∞ performance for a class of plants," *Syst. Control Lett.* **43**(3), 159–166 (2001).
[22] H. Hu, B. Jiang and H. Yang, "Non–fragile H_2 reliable control for switched linear systems with actuator faults," *Signal Process.* **93**(7), 1804–1812 (2013).
[23] R. Storn and K. Price, "Differential evolution—a simple and efficient heuristic for global optimization over continuous spaces," *J. Glob. Optim.* **11**, 341–359 (1997).
[24] R. Storn, "System design by constraint adaptation and differential evolution," *IEEE Trans. Evol. Comput.* 3(1), 22–34 (1999).
[25] W. Gong, Z. Cai, J. Yang, X. Li and L. Jian, "Parameter identification of an SOFC model with an efficient, adaptive differential evolution algorithm," *Int. J. Hydrogen Energy* **39**(10), 5083–5096 (2014).
[26] B. Liu, L. Wang, Y. H. Jin, D. X. Huang and F. Tang, "Control and synchronization of chaotic systems by differential evolution algorithm," *Chaos Solitons Fractals* **34**(2), 412–419 (2007).
[27] D. Ginoya, P. D. Shendge and S. B. Phadke, "Sliding mode control for mismatched uncertain systems using an extended disturbance observer," *IEEE Trans. Ind. Electron.* **61**(4), 1983–1992 (2014).
[28] D. Ginoya, P. D. Shendge and S. B. Phadke, "Disturbance observer based sliding mode control of nonlinear mismatched uncertain systems," *Commun. Nonlinear Sci. Numer. Simul.* **26**(1–3), 98–107 (2015).

https://doi.org/10.1017/S0263574721001776 Published online by Cambridge University Press

[29] X. Chen, H. Xu and M. Feng, "H_2 performance analysis and H_2 distributed control design for systems interconnected over an arbitrary graph," *Syst. Control Lett.* **124**, 1–11 (2019).
[30] J. R. Forbes, "Dual approaches to strictly positive real controller synthesis with a H_2 performance using linear matrix inequalities," *Int. J. Robust Nonlinear Control* **23**(8), 903–918 (2013).
[31] R. Lu, W. Du, J. Wang and A. Xue, "Robust H_2 control for descriptor system based on new bounded real lemma," *Circuits Syst. Signal Process.* **28**(6), 869–882 (2009).
[32] C. Scherer, P. Gahinet and M. Chilali, "Multiobjective output–feedback control via LMI optimization," *IEEE Trans. Autom. Control* **42**(7), 896–911 (1997).
[33] W. W. Zhang and J. Wang, "Nonsingular Terminal sliding model control based on exponential reaching law," *Control Decis.* **27**(6), 909–913 (2012).
[34] J. Liu, *Sliding Mode Control Design and MATLAB Simulation* (Tsinghua University press, Beijing, China, 2015).
[35] S. Skogestad, "Simple analytic rules for model reduction and PID controller tuning," *J. Process Control* **13**(4), 291–309 (2003).
[36] J. S. Fang, J. S. H. Tsai, J. J. Yan and S. M. Guo, "Robust sliding model control-based adaptive tracker for a class of nonlinear systems with input nonlinearities and uncertainties," *Trans. Inst. Meas. Control* **43**(7), 1629–1639 (2021).

Cite this article: S. Liu, G. Liu and S. Wu (2022). "Adaptive sliding tracking control for nonlinear uncertain robotic systems with unknown actuator nonlinearities", Robotica **40**, 2527–2546. https://doi.org/10.1017/S0263574721001776

https://doi.org/10.1017/S0263574721001776 Published online by Cambridge University Press